EXPERIMENTAL STUDY

Expression signatures of lncRNAs in skeletal muscles at the early flow phase revealed by microarray in burned rats

Zhang Haijun, M.D., Yu Yonghui, M.D., Chai Jiake, M.D.

Department of Burn and Plastic Surgery, First Affiliated Hospital of PLA General Hospital, Beijing, China

ABSTRACT

BACKGROUND: Severe thermal trauma covering more than 30% of the total body surface area (TBSA) triggers a sustained pathophysiological response, which includes, but is not limited to, hypermetabolism, chronic inflammation, and severe skeletal muscle wasting. Long non-coding RNAs (lncRNAs) are an important class of pervasive genes involved in a variety of biological functions. However, the functions of lncRNAs in the regulation of responses of skeletal muscle wasting after severe burn have remained untested.

METHODS: Presently examined were the expression profiles of lncRNAs and messenger RNAs (mRNAs) in skeletal muscle tissues of 3 pairs of burned rats at the early flow phase, compared with sham rats, using microarray. Each potential lncRNA-mRNA pair identified is a strong candidate in the definitive confirmation of the presence of specific lncRNA-mRNA interactions, thus providing a detailed picture of the pathogenesis of skeletal muscle wasting in burned rats.

RESULTS: LncRNA expression levels were compared among 3 injured tissues and matched normal tissues from microarray data. An average of 117 significantly differentially expressed lncRNAs (1.5-fold) were identified. Only 202 mRNAs were significantly upregulated or downregulated, an average of 92 mRNAs were upregulated in injured, compared to matched normal, tissues, while an average of 110 mRNAs) were downregulated.

CONCLUSION: Presently identified were lncRNAs differentially expressed in skeletal muscles of burned rats, compared to normal tissues. Regulatory pathways may be involved in the pathogenesis of skeletal muscle wasting. Each lncRNA-mRNA pair identified is a strong candidate for a future study to definitively confirm the presence of specific lncRNA-mRNA interactions, thus providing a more detailed picture of the pathogenesis of skeletal muscle wasting in burned rats.

Keywords: Burn; expression; LncRNAs; microarray; muscle wasting.

INTRODUCTION

Injuries represent one of the most important public health problems in economically developing and developed countries. Of the major types of injuries, burns contribute to more than 1% of the global burden of disease.[1–3] Burn injury is a primary cause of disability and mortality, with severe economic and social consequences. It can also lead to pain, as well as somatic and psychological complications.[1] Severe thermal trauma covering more than 30% of total body surface area (TBSA) triggers a sustained pathophysiological response, which includes, but is not limited to, hypermetabolism, chronic inflammation, marked elevations in peripheral catecholamines and cortisol levels, and severe skeletal muscle wasting.[2–4]

Severe burn injuries lead to a prolonged hypercatabolic state resulting in dramatic loss of skeletal muscle mass.[5] As skeletal muscle accounts for over 50% of the dry weight of the body's cells, its catabolism exerts a profound effect on the body's metabolism as a whole.[6] The primary mechanisms underlying skeletal muscle wasting induced by severe burn include activation of ubiquitin-proteasome pathway,[7,8] myonuclear apoptosis,[9] mitochondrial dysfunction,[10] autophagy,[11] signaling pathways driving muscle inflammation, and protein metabolism.[5] Although the mechanisms of skeletal muscle wasting following severe burn are becoming increasingly clear, the mechanisms of transcriptional and/or post-transcriptional gene regulation remain unknown.

Long non-coding RNAs (lncRNAs) have gained widespread attention in recent years as a potentially new and crucial layer of biological regulation.[12] LncRNAs have been implicated

Address for correspondence: Chai Jiake, M.D.
51 Fucheng Road Beijing - China
Tel: +86-10-6686-7972 E-mail: cjk304@126.com

Qucik Response Code

Ulus Travma Acil Cerrahi Derg
2016;22(3):224–232
doi: 10.5505/tjtes.2015.04831

in a wide range of developmental processes and diseases.[13] LncRNAs have emerged as key components of the address code, allowing protein complexes, genes, and chromosomes to be trafficked to appropriate locations, and subjected to proper activation and deactivation. LncRNA-based mechanisms control the fate of cells during development, and their dysregulation underlies some human disorders caused by chromosomal deletions and translocations.[14,15]

LncRNAs are generally longer than 200 nucleotides. Recent studies have shown that lncRNAs may act as important cis- or trans-regulators in various biological processes.[16] Mutations in lncRNAs are associated with a wide range of diseases, including stress, and particularly cancers and neurodegenerative diseases.[17] However, the profiles of burn-related lncRNAs have yet to be documented. Recent studies have shown that transcription of the mammalian genome is not only pervasive, but also enormously complex. It is estimated that an average of 10 transcription units, the vast majority of which make lncRNAs, may overlap with each traditional coding gene. These lncRNAs include antisense, and intronic and intergenic transcripts, as well as pseudogenes and retrotransposons.[18]

Presently examined are the expression profiles of lncRNAs and mRNAs in skeletal muscle tissues of 3 pairs of burned rats at the end of the shock phase, compared with sham rats, using microarray. Differentially expressed lncRNAs were then selected for target prediction with bioinformatics analyses. To improve the accuracy of target prediction, differentially expressed mRNAs were combined with target prediction of differentially expressed lncRNAs. The predicted target genes from the above analyses were subjected to bioinformatics analyses,[19] including gene ontology analysis, pathway analysis, and network analysis. Analyzing potential molecular markers and the possible relationship between differentially expressed lncRNAs and protein-coding genes in skeletal muscles at the early flow phase in burned rats will provide further insights into the pathogenesis of skeletal muscle wasting in thermal trauma.

MATERIALS AND METHODS

Sample Preparation

The present study was approved by the Committee of Science and Technology of the First Affiliated Hospital of PLA General Hospital, in accordance with the protocol outlined in the Guide for the Care and Use of Laboratory Animals published by the US National Institutes of Health (NIH publication no. 85-23, revised 1996).

Six adult male Wistar rats weighing 200–220 g each were purchased from the Chinese Medical Scientific Institute (Beijing, China). Rats were kept in controlled standard housing conditions with free access to standard laboratory food and water for a 7-day adaptation period before being randomly assigned to groups.

After fur was clipped, a full thickness thermal injury of 30% of TBSA was inflicted by immersing the back of the trunk in 94°C water for 12 seconds. A weight- and time-matched sham-burn group (n=3) was treated in the same manner as the trauma group (n=3), with the exception of the immersion of the sham-burn animals in room temperature water. During the post-burn period and following immersion, all rats were immediately dried, administered fluid (40 ml/kg of Ringer's lactate solution, calculated by the Parkland formula), and housed in individual cages with free access to food and water.[9] On the third day following burn or sham injury, the animals were euthanized. Tibialis anterior muscles were harvested and stored at -80°C for RNA extraction.

LncRNA and mRNA Microarray

Rat lncRNA array was designed for profiling lncRNA and protein-coding genes. Approximately 9,000 lncRNAs were selected from the NCBI Reference Sequence Database: all UCSC mRNA records and orthologs of rat lncRNAs. While probes for coding genes were printed once, probes for lncRNAs were printed 3 times. Probes for housekeeping genes and negative probes were printed multiple times to ensure hybridization quality.

RNA Labeling and Array Hybridization

Sample labeling and array hybridization were performed according to Agilent One-Color Microarray-Based Gene Expression Analysis Protocol (Agilent Technologies, Inc., Santa Clara, CA, USA). Briefly, total RNA from each sample was linearly amplified and labeled with Cy3-UTP. Labeled cRNAs were purified using the RNeasy Mini Kit (Qiagen, Inc., Hilden, Germany). Concentration and specific activity of labeled cRNAs (pmol Cy3/μg cRNA) were measured using the NanoDrop ND-1000 spectrophotometer (Thermo Fisher Scientific, Inc., Waltham, MA, USA). One μg of each labeled cRNA was fragmented by adding 11 μl of 10×blocking agent and 2.2 μl of 25×fragmentation buffer. The mixture was then heated at 60°C for 30 min, and finally, 55 μl of 2×GE hybridization buffer was added to dilute the labeled cRNA. A total of 100 μl of hybridization solution was dispensed into the gasket slide and assembled onto the gene expression microarray slide. The slides were incubated at 65°C for 17 hours in an Agilent hybridization oven (Agilent Technologies, Inc., Santa Clara, CA, USA). The hybridized arrays were washed, fixed, and scanned using an Agilent DNA microarray scanner (part no. G2505C; Agilent Technologies, Inc., Santa Clara, CA, USA).

Data Analysis

Agilent Feature Extraction software (version 11.0.1.1; Agilent Technologies, Inc., Santa Clara, CA, USA) was used to analyze the acquired array images. Quantile normalization and subsequent data processing were performed using GeneSpring GX version 12.0 software package (Agilent Technologies, Inc., Santa Clara, CA, USA). Following quantile normalization of the raw data, lncRNAs and mRNAs for which at least 3 out

of 6 samples had flags in "Present" or "Marginal" ("All Targets Value") were chosen for further data analysis.

Differentially expressed lncRNAs and mRNAs with statistical significance were identified using volcano plot filtering. Hierarchical clustering was performed using GeneSpring GX software (version 12.0; Agilent Technologies, Inc., Santa Clara, CA, USA).

Construction of the Coding-Non-Coding Gene Co-Expression Network

To show that the lncRNAs directly regulated the expression of target mRNAs, lncRNA target predictions were superimposed onto the lncRNA-mRNA correlation network. The resulting network was defined as an lncRNA-mRNA regulatory network. A direct connection was placed from an lncRNA to an mRNA using either a blue line (trans-interaction) or a red line (cis-interaction).

Statistical Analysis

Results were expressed as mean±SD. Statistical analysis was performed using Student's t-test for comparison of 2 groups in the microarray, and analysis of variance was used for multiple comparisons. In both cases, differences with $p<0.05$ were considered to be statistically significant. Statistical significance of microarray results was analyzed by fold change and Student's t-test. False discovery rate was calculated in order to correct p values. The threshold value used to screen differentially expressed lncRNAs and mRNAs was a fold change ≥1.5 ($p<0.05$).

Table 1. Upregulated lncRNA profiles

Probe name	p value	Fold change and regulation		Probe name	p value	Fold change and regulation	
		Absolute fold change ([T] vs [C])	Regulation ([T] vs [C])			Absolute fold change ([T] vs [C])	Regulation ([T] vs [C])
XR_007625_P1	0.042436516	1.513741298	up	S75669_P1	0.007335414	1.939438731	up
XR_008295_P1	0.006886517	1.608696682	up	S75669_P1	0.007335414	1.939438731	up
MRAK080815_P1	0.020947862	1.520309795	up	S75669_P1	0.007335414	1.939438731	up
XR_005515_P1	0.040546402	1.626680595	up	S75669_P1	0.007335414	1.939438731	up
XR_009083_P1	0.006434708	1.617928104	up	XR_009355_P1	0.048364759	1.556603421	up
XR_006772_P1	0.038080035	1.549397303	up	XR_005513_P1	0.006641351	1.75941563	up
XR_005733_P1	0.01100545	1.551780677	up	XR_006841_P1	0.028879691	1.564961501	up
XR_007062_P1	0.003142118	1.914118172	up	AY643514_P1	0.033154207	1.503992702	up
XR_007206_P1	0.024360851	2.084225919	up	AY643514_P1	0.033154207	1.503992702	up
MRAK142335_P1	0.043959593	1.955781634	up	XR_006694_P1	0.006682623	1.691703812	up
MRuc007guc_P1	0.026266496	1.93846981	up	MRAK053201_P1	0.049504017	1.694329931	up
XR_006148_P1	0.012795552	1.640795758	up	DQ832324_P1	0.01193803	1.604519178	up
AF332363_P1	0.009779	1.767327041	up	XR_008093_P1	0.005252984	1.622082653	up
XR_007393_P1	0.042234037	1.836920259	up	XR_005488_P1	0.049406948	1.739175513	up
MRAK040107_P1	0.034288649	1.743452026	up	XR_009151_P1	0.034915223	1.514451804	up
MRAK040107_P1	0.034288649	1.743452026	up	XR_005800_P1	0.001871706	1.715524821	up
BC098776_P1	0.005731768	1.543092558	up	uc.152-_P1	0.04315685	1.713979119	up
XR_006678_P1	0.042567859	1.708809769	up	XR_008501_P1	0.023420274	1.61734673	up
MRAK012222_P1	0.018538406	1.592452676	up	XR_007720_P1	0.014669486	1.727730824	up
XR_006337_P1	0.023330015	1.736155055	up	XR_006550_P1	0.002260132	1.531738302	up
XR_007784_P1	0.010820094	1.541399506	up	XR_005754_P1	0.006875391	1.819631944	up
XR_006785_P1	0.009177714	1.647233223	up	XR_007321_P1	0.011698519	1.673666406	up
MRAK006088_P1	0.047430249	1.535065022	up	XR_008911_P1	0.014100815	1.593491511	up
MRAK006088_P1	0.047430249	1.535065022	up	MRAK004125_P1	0.012228179	1.50735389	up
MRAK032396_P1	0.002439049	1.745553893	up	BC168236_P1	0.033712827	2.592948166	up
MRAK032396_P1	0.002439049	1.745553893	up	MRAK032113_P1	0.025968499	1.865618242	up
XR_006529_P1	0.005485356	1.651250693	up	XR_007247_P1	0.013873027	1.574192895	up
MRAK145223_P1	0.028223934	1.904590841	up	AY383698_P1	0.042209102	1.525491351	up
XR_006328_P1	0.022030979	1.550920784	up	AY383698_P1	0.042209102	1.525491351	up
MRAK135387_P1	0.019185074	1.501364733	up	MRAK131727_P1	0.034235162	1.513193901	up
XR_005665_P1	0.041147848	2.239151018	up	XR_005772_P1	0.035771322	1.533147498	up
S75669_P1	0.007335414	1.939438731	up	D26496_P1	0.043220295	1.510179878	up

#Fold change cut-off: 1.5; #p value cut-off: 0.05; #Condition pairs: T vs C.

RESULTS

Overview of Expression Profiles of lncRNAs

From the lncRNA expression profiles, differentially expressed lncRNAs were found from among samples of skeletal muscles obtained from thermal rats (thermal group) and sham-burn rats (control group). Expression profiles of lncRNAs in paired samples were shown by calculating log-fold change of the thermal group/the control group (T/C). Agreement was formulated as follows: fold change cut-off was 1.5, and for any fold change, positive value indicated upregulation, while negative value indicated downregulation. Log-fold change signified log2 value of absolute fold change. Fold change and p values were calculated from the normalized expression.

LncRNA expression levels were compared among the 3 injured tissues and their matched normal tissues from the microarray data, and an average of 117 long lncRNAs that were significantly differentially expressed (1.5-fold) were identified. Results demonstrated that a very large number of lncRNAs could be examined in normal and injured tissues, while only 117 of these were significantly upregulated (Table 1) or downregulated (Table 2), and could be used to discriminate skeletal muscles of burned rats from matched normal tissues. Compared to the normal tissues, MRAK080917 (log2 fold change T/C=6.777752082) was most significantly downregulated, while BC168236 (log2 fold change T/C=2.592948166) was most significantly upregulated. It was determined that downregulated lncRNAs were more common than those that were upregulated.

Overview of mRNA Profiles

Results demonstrated that tens of thousands of mRNAs could be examined in normal and injured tissues, but that only 202 mRNAs were significantly upregulated or downregulated. An average of 92 mRNAs were upregulated in the injured tissues (Table 3), compared to the matched normal ones, while an average of 110 mRNAs were downregulated (Table 4).

Table 2. Downregulated lncRNA profiles

Probe name	p value	Fold change and regulation		Probe name	p value	Fold change and regulation	
		Absolute fold change ([T] vs [C])	Regulation ([T] vs [C])			Absolute fold change ([T] vs [C])	Regulation ([T] vs [C])
MRAK15842	5.30947E-05	2.397271208	down	uc.414+_P1	0.035614403	1.742281172	down
MRAK05384	0.047353911	1.826165856	down	XR_008292_	0.002067679	1.683021803	down
BC088246_P1	0.010256908	1.691622866	down	BC088244_P1	0.016885746	1.559107747	down
MRAK01357	0.049684039	2.110840155	down	XR_006390_	0.03336485	1.666808775	down
XR_005853_	0.012668374	1.995183722	down	XR_007170_	0.031927225	1.504417159	down
XR_007420_	0.044076153	1.932416621	down	MRAK01401	0.047898874	1.861431079	down
MRAK13343	0.046766231	1.741470861	down	BC091431_P1	0.040444159	1.774696923	down
XR_008004_	0.049786366	1.564872337	down	MRNR_0274	0.043534745	1.520794796	down
XR_007008_	0.027827377	1.586787642	down	MRNR_0274	0.043534745	1.520794796	down
XR_009508_	0.010834758	1.621010085	down	MRAK08854	0.034608972	1.594106481	down
MRuc008lum	0.046532415	1.731525939	down	MRAK13756	0.049387275	2.266269552	down
MRBC05287	0.036183082	1.986867961	down	XR_006360_	0.031595041	1.992246736	down
MRAK01247	0.035900857	1.627108736	down	XR_005641_	0.010076191	1.875123347	down
XR_006437_	0.035308453	1.655361222	down	MRuc007lsc	0.010926997	1.779102256	down
XR_006093_	0.044244767	1.578948628	down	MRAK04093	0.033756148	2.464227295	down
L27129_P1	0.011395706	1.840498533	down	MRAK08024	0.03462557	2.578548176	down
MRuc008ras	0.043368383	1.651454361	down	uc.392+_P1	0.030557302	1.897403964	down
XR_008415_	0.009885108	3.936073061	down	XR_007260_	0.027345191	1.87398062	down
uc.292+_P1	0.033380577	1.544869528	down	BC129118_P1	0.049050374	1.795345078	down
MRAK16128	0.006865299	1.704064842	down	BC105769_P1	0.036040215	1.532308552	down
BC161881_P1	0.000525852	2.903724206	down	MRBC02501	0.02883171	1.84676539	down
MRAK17259	0.047606367	1.505013888	down	MRAK08082	0.003419968	1.688903112	down
XR_005949_	0.029279799	1.740566901	down	BC091254_P1	0.043449559	1.774148166	down
XR_006777_	0.044210245	1.586528935	down	MRAK03323	0.022282206	2.550611731	down
MRAK08091	0.018362991	6.777752082	down	MRAK08884	0.013406108	1.688892108	down
uc.414+_P1	0.035614403	1.742281172	down	MRAK03718	0.018860453	2.452178953	down
uc.414+_P1	0.035614403	1.742281172	down				

#Fold change cut-off: 1.5; #p value cut-off: 0.05; #Condition pairs: T vs C.

Construction of the Coding-Non-Coding Gene Co-Expression Network

A coding-non-coding gene co-expression network (CNC network) was constructed based on correlation analysis of the differentially expressed lncRNAs and mRNAs (Figure 1). LncRNAs and mRNAs with Pearson's correlation coefficients not less than 0.99 were selected to draw the network, using the Cytoscape program (Institute of Systems Biology, Seattle,

Table 3. Upregulated mRNA profiles

Probe name	p value	Fold change and regulation		Probe name	p value	Fold change and regulation	
		Absolute fold change ([T] vs [C])	Regulation ([T] vs [C])			Absolute fold change ([T] vs [C])	Regulation ([T] vs [C])
CUST_1210_PI421866198	0.045606394	1.59759874	up	CUST_11657_PI421866198	0.012815076	2.177136405	up
CUST_10195_PI421866198	0.010355438	5.063922528	up	CUST_7560_PI421866198	0.040101847	1.65046247	up
CUST_1855_PI421866198	0.00137129	2.617241527	up	CUST_10534_PI421866198	0.01945795	1.628197076	up
CUST_2486_PI421866198	0.020719392	1.90840495	up	CUST_13435_PI421866198	0.037294419	2.018765962	up
CUST_4642_PI421866198	0.029708762	1.654661374	up	CUST_3946_PI421866198	0.00503991	2.915539092	up
CUST_6944_PI421866198	0.007240272	4.257326589	up	CUST_4654_PI421866198	0.001786365	3.507455905	up
CUST_15260_PI421866198	0.000577946	1.563042132	up	CUST_10867_PI421866198	0.039276132	2.023074619	up
CUST_5342_PI421866198	0.037533375	2.430356579	up	CUST_11542_PI421866198	0.001880145	3.595193945	up
CUST_11829_PI421866198	0.0100799	3.253144336	up	CUST_874_PI421866198	0.03049041	1.549625107	up
CUST_15262_PI421866198	0.00574348	2.040395513	up	CUST_6327_PI421866198	0.019006624	1.656331373	up
CUST_2300_PI421866198	0.043473392	2.041859786	up	CUST_10004_PI421866198	0.009444256	1.801275848	up
CUST_10432_PI421866198	0.014915171	3.255336544	up	CUST_2643_PI421866198	0.042958202	1.611518406	up
CUST_7003_PI421866198	0.005680592	1.966802326	up	CUST_12088_PI421866198	0.007111663	4.217454975	up
CUST_5856_PI421866198	0.00444493	1.514130444	up	CUST_11522_PI421866198	0.016947821	1.526485621	up
CUST_3262_PI421866198	0.011125493	1.626468671	up	CUST_7763_PI421866198	0.044559992	2.452112778	up
CUST_3486_PI421866198	0.026690711	1.861147332	up	CUST_9248_PI421866198	0.021534995	1.573094493	up
CUST_4557_PI421866198	0.032782771	2.377418854	up	CUST_10991_PI421866198	0.033401846	2.651287522	up
CUST_13837_PI421866198	0.036516598	1.518998312	up	CUST_654_PI421866198	0.011979725	1.904043361	up
CUST_7855_PI421866198	0.013731288	2.031357834	up	CUST_11606_PI421866198	0.035018534	2.611823367	up
CUST_9330_PI421866198	0.002192444	1.821304992	up	CUST_14500_PI421866198	0.011436587	2.178194373	up
CUST_8448_PI421866198	0.03433747	2.348021686	up	CUST_1791_PI421866198	0.012327838	1.685268466	up
CUST_7759_PI421866198	0.030562675	2.302327658	up	CUST_10895_PI421866198	0.002460083	1.803186767	up
CUST_8107_PI421866198	0.039949858	1.817725142	up	CUST_2059_PI421866198	0.016699039	4.0862396	up
CUST_13967_PI421866198	0.011714172	1.502536808	up	CUST_12802_PI421866198	0.001146504	1.959951788	up
CUST_13858_PI421866198	0.031802356	4.327122709	up	CUST_14787_PI421866198	0.021016027	1.847760579	up
CUST_3094_PI421866198	0.049342616	1.559352399	up	CUST_12797_PI421866198	0.043673356	1.626239603	up
CUST_4831_PI421866198	0.009792921	3.028942659	up	CUST_3027_PI421866198	0.038742155	2.095886609	up
CUST_9367_PI421866198	0.002270001	1.504368323	up	CUST_3860_PI421866198	0.006603383	2.072462648	up
CUST_12576_PI421866198	0.021936529	1.530467349	up	CUST_9836_PI421866198	0.046263826	2.805332937	up
CUST_11559_PI421866198	0.037735196	1.586725757	up	CUST_6100_PI421866198	0.023983273	1.646977676	up
CUST_10215_PI421866198	0.020469822	1.987755392	up	CUST_9174_PI421866198	0.044585762	1.572939157	up
CUST_862_PI421866198	0.029139124	1.62620372	up	CUST_9559_PI421866198	0.00320455	1.85037819	up
CUST_11044_PI421866198	0.043897171	2.412127444	up	CUST_12615_PI421866198	0.044961697	5.12824374	up
CUST_11815_PI421866198	0.008441526	3.050925744	up	CUST_12694_PI421866198	0.000445438	6.02873591	up
CUST_12246_PI421866198	0.03359414	1.950991285	up	CUST_5146_PI421866198	0.029780754	3.435343433	up
CUST_13854_PI421866198	0.042522872	2.037577641	up	CUST_14214_PI421866198	0.022183257	1.906633522	up
CUST_8809_PI421866198	0.017832572	2.054859613	up	CUST_5814_PI421866198	0.019676952	2.119471646	up
CUST_2710_PI421866198	0.002845954	8.341076172	up	CUST_5887_PI421866198	0.04427284	1.726615686	up
CUST_3992_PI421866198	0.037372541	1.584239441	up	CUST_9879_PI421866198	0.026613386	3.480238877	up
CUST_3166_PI421866198	0.00670917	1.673006325	up	CUST_10303_PI421866198	0.03072874	4.236377053	up
CUST_6053_PI421866198	0.046093471	1.731258715	up	CUST_5232_PI421866198	0.019294662	1.711679983	up
CUST_11231_PI421866198	0.036003194	1.665044421	up	CUST_539_PI421866198	0.034040423	2.229217679	up
CUST_7773_PI421866198	0.036907358	1.608969152	up	CUST_1893_PI421866198	0.010545646	1.566298301	up
CUST_8733_PI421866198	0.015020579	1.695315831	up	CUST_2513_PI421866198	0.02086206	2.028827679	up
CUST_6940_PI421866198	0.036482366	1.644952586	up	CUST_2838_PI421866198	0.019319005	1.660433334	up
CUST_1492_PI421866198	0.037677048	1.765124567	up	CUST_370_PI421866198	0.000366622	1.907148258	up

Table 4. Downregulated mRNA profiles

Probe name	p value	Fold change and regulation		Probe name	p value	Fold change and regulation	
		Absolute fold change ([T] vs [C])	Regulation ([T] vs [C])			Absolute fold change ([T] vs [C])	Regulation ([T] vs [C])
CUST_4198_PI421866198	0.0067783	1.628791683	down	CUST_7536_PI421866198	0.049372269	1.895256483	down
CUST_776_PI421866198	0.007212239	1.814502444	down	CUST_9125_PI421866198	0.012439588	2.087408269	down
CUST_10318_PI421866198	0.02131578	3.252387526	down	CUST_11390_PI421866198	0.048161951	2.326862939	down
CUST_7779_PI421866198	0.033695322	1.75749043	down	CUST_10258_PI421866198	0.037506169	1.684580066	down
CUST_3858_PI421866198	0.003915407	1.539287448	down	CUST_11901_PI421866198	0.031870641	1.941909095	down
CUST_1082_PI421866198	0.029269283	1.585292074	down	CUST_3360_PI421866198	0.024288361	1.964775215	down
CUST_4192_PI421866198	0.013624005	1.502800985	down	CUST_3248_PI421866198	0.01717798	1.65095485	down
CUST_14720_PI421866198	0.044151095	1.983600187	down	CUST_11572_PI421866198	0.042170403	1.623829696	down
CUST_10036_PI421866198	0.015626469	1.605582355	down	CUST_13054_PI421866198	0.010350555	2.672858999	down
CUST_5668_PI421866198	0.008412707	1.549091469	down	CUST_9107_PI421866198	0.039358033	2.054262673	down
CUST_11039_PI421866198	0.022341275	4.302450915	down	CUST_10023_PI421866198	0.033561008	1.872143645	down
CUST_12190_PI421866198	0.038150892	2.184822485	down	CUST_8571_PI421866198	0.024507169	1.931788968	down
CUST_7670_PI421866198	0.030325542	1.786994631	down	CUST_6493_PI421866198	0.016041024	1.534768436	down
CUST_6411_PI421866198	0.02170252	4.228192419	down	CUST_4967_PI421866198	0.016405071	1.732526997	down
CUST_9295_PI421866198	0.012044678	5.265246349	down	CUST_9652_PI421866198	0.038653891	1.698414312	down
CUST_333_PI421866198	0.02729877	2.068126692	down	CUST_11024_PI421866198	0.041375285	1.585211494	down
CUST_7231_PI421866198	0.045267906	1.988425486	down	CUST_11380_PI421866198	0.023145073	1.972866179	down
CUST_2560_PI421866198	0.049736128	2.029461915	down	CUST_4567_PI421866198	0.000735864	1.609649972	down
CUST_33_PI421866198	0.014357628	1.634448213	down	CUST_8200_PI421866198	0.015255319	1.854687725	down
CUST_9028_PI421866198	0.003902698	1.500420452	down	CUST_5928_PI421866198	0.034725016	1.649610019	down
CUST_14308_PI421866198	0.007826484	1.599796943	down	CUST_14935_PI421866198	0.012652676	1.777394587	down
CUST_8516_PI421866198	0.026925455	1.545754637	down	CUST_8147_PI421866198	0.047774903	2.512465466	down
CUST_3482_PI421866198	0.027384736	1.56126868	down	CUST_11318_PI421866198	0.024469389	1.801610366	down
CUST_6919_PI421866198	0.023519185	2.867930507	down	CUST_12570_PI421866198	0.0199879	6.164450222	down
CUST_2509_PI421866198	0.041171198	2.197500256	down	CUST_9797_PI421866198	0.018976082	2.905925735	down
CUST_5357_PI421866198	0.005533369	2.464244091	down	CUST_13012_PI421866198	0.044403789	1.566228458	down
CUST_383_PI421866198	0.005899414	2.043783909	down	CUST_2160_PI421866198	0.023758555	1.875550749	down
CUST_6065_PI421866198	0.033150212	3.01190688	down	CUST_6349_PI421866198	0.009680624	1.664260649	down
CUST_11240_PI421866198	0.009535117	1.604777926	down	CUST_609_PI421866198	0.039611572	2.048383439	down
CUST_5578_PI421866198	0.022595551	1.518187137	down	CUST_5091_PI421866198	0.029473561	1.741826508	down
CUST_101_PI421866198	0.024100642	1.732010889	down	CUST_9434_PI421866198	0.016207278	1.699652485	down
CUST_1302_PI421866198	0.010298785	3.640830473	down	CUST_14233_PI421866198	0.025889633	1.830465522	down
CUST_8391_PI421866198	0.019406484	1.678849454	down	CUST_1862_PI421866198	0.043523032	1.989012487	down
CUST_4319_PI421866198	0.018043175	1.591434007	down	CUST_2828_PI421866198	0.012457514	2.296501406	down
CUST_5514_PI421866198	0.021748994	2.160062964	down	CUST_3303_PI421866198	0.000785041	1.634238713	down
CUST_12018_PI421866198	0.043888152	2.505456518	down	CUST_7885_PI421866198	0.019408921	1.61555388	down
CUST_14802_PI421866198	0.047467746	2.091477871	down	CUST_6904_PI421866198	0.031971115	1.687945512	down
CUST_12841_PI421866198	0.015876313	2.924250563	down	CUST_9084_PI421866198	0.020976626	1.633773816	down
CUST_4276_PI421866198	0.037379472	1.541802423	down	CUST_10372_PI421866198	0.034163437	1.531920752	down
CUST_4886_PI421866198	0.028589317	1.645704145	down	CUST_6343_PI421866198	0.02350771	1.591532443	down
CUST_7724_PI421866198	0.026010169	1.700709814	down	CUST_9900_PI421866198	0.009545992	1.627704149	down
CUST_1736_PI421866198	0.034807531	1.527727959	down	CUST_2923_PI421866198	0.01879922	1.526455819	down
CUST_3184_PI421866198	0.027050956	1.67183407	down	CUST_3414_PI421866198	0.045886349	1.728345527	down
CUST_5601_PI421866198	0.000686672	1.52572276	down	CUST_9269_PI421866198	0.030872404	1.795461851	down
CUST_584_PI421866198	0.044594505	1.623093751	down	CUST_1731_PI421866198	0.004534508	1.519119469	down
CUST_12238_PI421866198	0.001505492	1.510598473	down	CUST_14236_PI421866198	0.000522689	2.343916593	down
CUST_6202_PI421866198	0.034681376	1.680710099	down	CUST_14943_PI421866198	0.041784213	1.52157488	down
CUST_5030_PI421866198	0.047914238	1.735625876	down	CUST_9835_PI421866198	0.009566858	1.549027046	down
CUST_14123_PI421866198	0.00919136	1.793223113	down	CUST_1976_PI421866198	0.037596345	1.768400442	down
CUST_5098_PI421866198	0.037846355	1.676871727	down	CUST_5440_PI421866198	0.003370002	1.966515649	down
CUST_12249_PI421866198	0.035589358	1.693185845	down	CUST_601_PI421866198	0.008108411	1.546657228	down
CUST_14318_PI421866198	0.039627075	1.887104087	down	CUST_596_PI421866198	0.03101802	1.518329418	down
CUST_12907_PI421866198	0.030763082	1.553773667	down	CUST_8394_PI421866198	0.020034374	1.596096633	down
CUST_6039_PI421866198	0.047285771	1.537592638	down	CUST_8563_PI421866198	0.027774993	2.714663103	down
CUST_19_PI421866198	0.042225177	1.832891771	down	CUST_6633_PI421866198	0.006083932	1.746328538	down

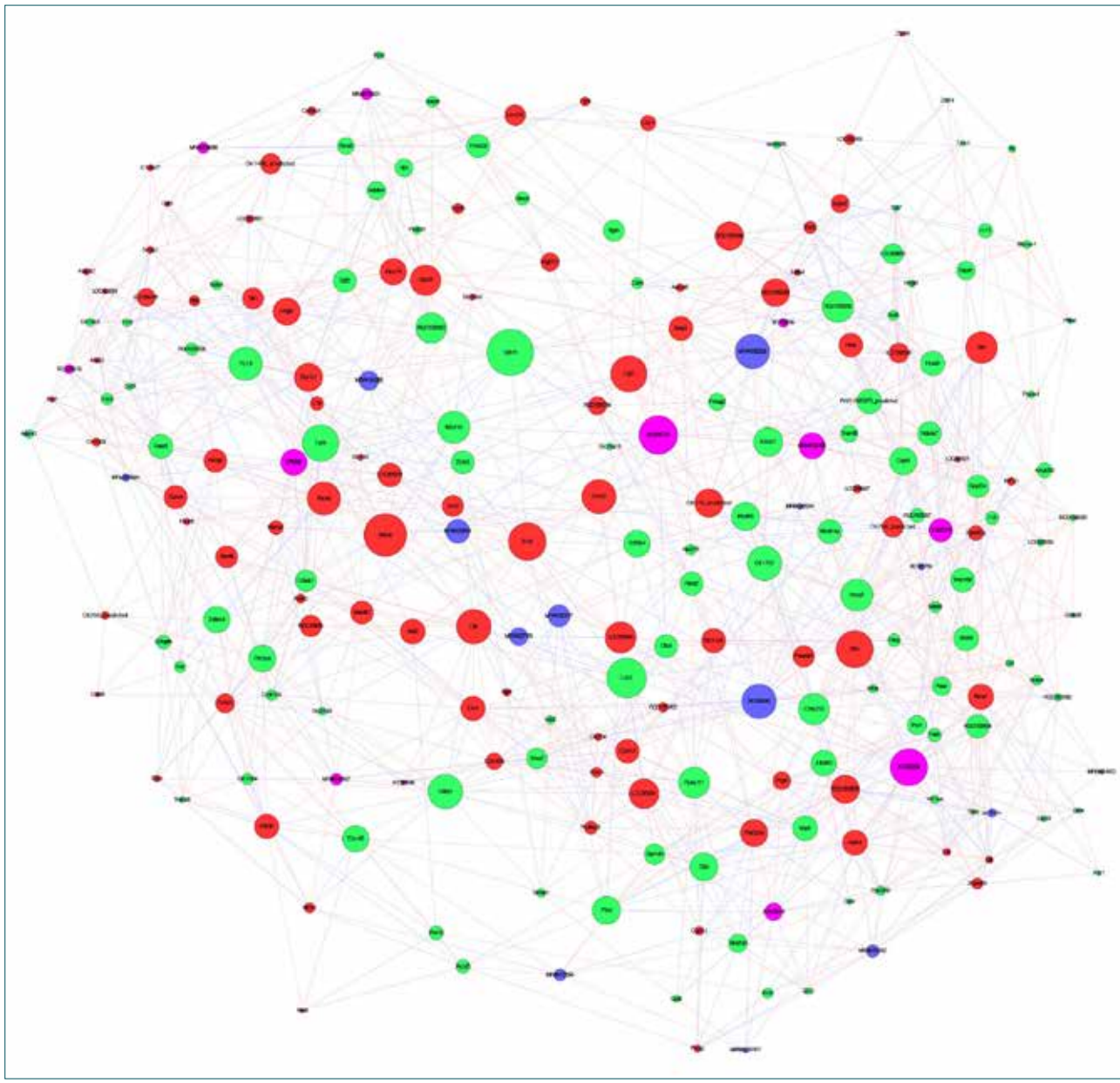

Figure 1. Predicted regulation network. A coding-non-coding gene co-expression network.
Node color: Upregulated lncRNAs: purple; Downregulated lncRNAs: blue; Upregulated mRNAs: red; Downregulated mRNAs: green.
Node size: Betweenness centrality (equal to the number of shortest paths from all vertices to all others that pass through that node).
Line color: Trans interaction: blue; Cis interaction: red; Cut-off: abs(correlation) >=0.95.

WA, USA); 117 lncRNAs and 202 mRNAs comprised the CNC network node. A total of 319 network nodes made 1392 associated network pairs of co-expressed lncRNAs and mRNAs. The CNC network indicated that one mRNA could correlate with 1 to several lncRNAs, and vice versa. The CNC network presented in Table S9 could implicate the inter-regulation of lncRNAs and mRNAs in burned rats.

DISCUSSION

Skeletal muscle wasting is an exacerbating factor in the prognosis of critically ill patients, including those with severe burn injury.[11] Molecular treatment mechanisms of skeletal muscle wasting in burn injuries have been extensively studied. However, the pathogenesis and gene regulation involved are still unknown.

Increasing evidence has confirmed lncRNAs to be one of the most important factors controlling gene expression.[20] Therefore, the lncRNA expression profile in the skeletal muscle tissue of burned rats was presently evaluated in an attempt to reveal the potential role of lncRNAs in the pathogenesis of skeletal muscle wasting in burn injury (Tables 1, 2). Microarray analyses revealed a set of differentially expressed lncRNAs, with 64 upregulated and 53 downregulated

lncRNAs in skeletal muscles of burned rats, when compared to normal tissue.

Recent studies have demonstrated that lncRNAs can guide changes in gene expression in either the cis (neighboring genes) or trans (distantly located genes) manner, which is not easily predicted, based on lncRNA sequence.[21] In principle, lncRNAs can guide chromatin change in cis in a cotranscriptional manner (tethered by RNA polymerase) or as a complementary target for small regulatory RNAs. Guidance in trans can occur by an lncRNA binding to target DNA as an RNA:DNA heteroduplex, RNA:DNA:DNA triplex, or by RNA recognition of a complex surface of specific chromatin features.[22]

The established role of lncRNAs in diseases creates an urgency to understand the mechanisms by which these RNAs seek their targets. A simplistic model in which the RNA remains tethered to the site of origin to regulate transcriptional changes in cis has been suggested. Perhaps the most intensely studied and best understood cis mechanism of regulation by lncRNA is the mammalian X inactivation center, a genetic locus that specifies a number of lncRNAs, including X-inactivation–specific transcript, or XIST.[21] Target genes under cis mechanism of regulation by lncRNAs were predicted via genome browser and annotation tool.

Further investigation of the lncRNA-gene network in an effort to gain insight into the functions of lncRNA targets demonstrated that MRAK080917 was predicted to target the Zbtb16 genes of the glioma pathway, which could affect total body weight, adiposity, lipid profile, insulin sensitivity of skeletal muscles, and mitochondrial function in skeletal muscles.[23,24] Uc.414+ was predicted to target THRA and Nr1d1. THRA is downregulated in skeletal muscle of patients with non-thyroidal illness syndrome secondary to non-septic shock,[25] while Nr1d1 could modulate skeletal muscle oxidative capacity by regulating mitochondrial biogenesis and autophagy.[26] MRBC025014 was predicted to target Sucla2, which is involved in mitochondrial disorder and progressive dystonia.[27,28]

Conclusions

In conclusion, lncRNAs differentially expressed in skeletal muscles of burned rats, compared to normal tissues, were identified in the present study. Regulatory pathways of lncRNAs may be involved in the pathogenesis of skeletal muscle wasting. Moreover, MRAK080917, uc.414+, and MRBC025014 could be critical in skeletal muscle wasting, via their targets, but these findings need to be confirmed, and the underlying mechanisms require further study. The present results also point to several exciting directions for future research. The CNC network presented in Table S9 implicated the inter-regulation of lncRNAs and mRNAs in burned rats. Each potential lncRNA-mRNA pair identified is a strong candidate for a future study that can definitively confirm the presence of specific lncRNA-mRNA interactions,[29] thus providing a more detailed picture of the pathogenesis of skeletal muscle wasting in burned rats.

Acknowledgments

This study was financially supported by the National Natural Science Foundation of China (81120108041, 81471873, 81171807) and the State Key Program of the General Logistics Department of the PLA (BWS14J048, BWS14J049). The authors wish to thank Kang Cheng Bio-tech Shanghai P.R. China for the microarray work.

Conflict of interest: None declared.

REFERENCES

1. Mohammadi-Barzelighi H1, Alaghehbandan R, Motevallian A, Alinejad F, Soleimanzadeh-Moghadam S, Sattari M, et al. Epidemiology of severe burn injuries in a Tertiary Burn Centre in Tehran, Iran. Ann Burns Fire Disasters 2011;24:59–62.
2. Porter C, Hurren NM, Herndon DN, Børsheim E. Whole body and skeletal muscle protein turnover in recovery from burns. Int J Burns Trauma 2013;3:9–17.
3. Jeschke MG, Gauglitz GG, Kulp GA, Finnerty CC, Williams FN, Kraft R, et al. Long-term persistance of the pathophysiologic response to severe burn injury. PLoS One. 2011;6:e21245. Crossref
4. Chai J, Wu Y, Sheng ZZ. Role of ubiquitin-proteasome pathway in skeletal muscle wasting in rats with endotoxemia. Crit Care Med 2003;31:1802–7. Crossref
5. Merritt EK, Cross JM, Bamman MM. Inflammatory and protein metabolism signaling responses in human skeletal muscle after burn injury. J Burn Care Res 2012;33:291–7. Crossref
6. Chai JK. Mechanisms of skeletal muscle wasting after severe burn and its treatment. [Article in Chinese] Zhonghua Shao Shang Za Zhi 2009;25:243–5.
7. Lagirand-Cantaloube J, Cornille K, Csibi A, Batonnet-Pichon S, Leibovitch MP, Leibovitch SA. Inhibition of atrogin-1/MAFbx mediated MyoD proteolysis prevents skeletal muscle atrophy in vivo. PLoS One 2009;4:e4973. Crossref
8. Sheriff S, Kadeer N, Joshi R, Friend LA, James JH, Balasubramaniam A. Des-acyl ghrelin exhibits pro-anabolic and anti-catabolic effects on C2C12 myotubes exposed to cytokines and reduces burn-induced muscle proteolysis in rats. Mol Cell Endocrinol 2012;351:286–95. Crossref
9. Duan H, Chai J, Sheng Z, Yao Y, Yin H, Liang L, et al. Effect of burn injury on apoptosis and expression of apoptosis-related genes/proteins in skeletal muscles of rats. Apoptosis 2009;14:52–65. Crossref
10. Tzika AA, Mintzopoulos D, Mindrinos M, Zhang J, Rahme LG, Tompkins RG. Microarray analysis suggests that burn injury results in mitochondrial dysfunction in human skeletal muscle. Int J Mol Med 2009;24:387–92. Crossref
11. Hosokawa S, Koseki H, Nagashima M, Maeyama Y, Yomogida K, Mehr C, et al. Title efficacy of phosphodiesterase 5 inhibitor on distant burn-induced muscle autophagy, microcirculation, and survival rate. Am J Physiol Endocrinol Metab 2013;304:922–33. Crossref
12. Zhang J, Cui X, Shen Y, Pang L, Zhang A, Fu Z, et al. Distinct expression profiles of LncRNAs between brown adipose tissue and skeletal muscle. Biochem Biophys Res Commun 2014;443:1028–34. Crossref
13. Batista PJ, Chang HY. Long noncoding RNAs: cellular address codes in development and disease. Cell 2013;152:1298–307. Crossref

14. Kung JT, Colognori D, Lee JT. Long noncoding RNAs: past, present, and future. Genetics 2013;193:651–69. Crossref
15. Lee JT, Bartolomei MS. X-inactivation, imprinting, and long noncoding RNAs in health and disease. Cell 2013;152:1308–23. Crossref
16. Ma H, Hao Y, Dong X, Gong Q, Chen J, Zhang J, et al. Molecular mechanisms and function prediction of long noncoding RNA. ScientificWorldJournal 2012;2012:541786. Crossref
17. Mizutani R, Wakamatsu A, Tanaka N, Yoshida H, Tochigi N, Suzuki Y, et al. Identification and characterization of novel genotoxic stress-inducible nuclear long noncoding RNAs in mammalian cells. PLoS One 2012;7:e34949. Crossref
18. Lee JT. Epigenetic regulation by long noncoding RNAs. Science 2012;338:1435–9. Crossref
19. Li JP, Liu LH, Li J, Chen Y, Jiang XW, Ouyang YR, et al. Microarray expression profile of long noncoding RNAs in human osteosarcoma. Biochem Biophys Res Commun 2013;433:200,6.
20. Khachane AN, Harrison PM. Mining mammalian transcript data for functional long non-coding RNAs. PLoS One 2010;5:e10316. Crossref
21. Hung T, Chang HY. Long noncoding RNA in genome regulation: prospects and mechanisms. RNA Biol 2010;7:582–5. Crossref
22. Pauli A, Rinn JL, Schier AF. Non-coding RNAs as regulators of embryogenesis. Nat Rev Genet 2011;12:136–49. Crossref
23. Seda O, Liska F, Sedová L, Kazdová L, Krenová D, Kren V. A 14-gene region of rat chromosome 8 in SHR-derived polydactylous congenic substrain affects muscle-specific insulin resistance, dyslipidaemia and visceral adiposity. Folia Biol (Praha) 2005;51:53–61.
24. Plaisier CL, Bennett BJ, He A, Guan B, Lusis AJ, Reue K, et al. Zbtb16 has a role in brown adipocyte bioenergetics. Nutr Diabetes 2012;2:e46.
25. Lado-Abeal J, Romero A, Castro-Piedras I, Rodriguez-Perez A, Alvarez-Escudero J. Thyroid hormone receptors are down-regulated in skeletal muscle of patients with non-thyroidal illness syndrome secondary to non-septic shock. Eur J Endocrinol 2010;163:765–73. Crossref
26. Woldt E, Sebti Y, Solt LA, Duhem C, Lancel S, Eeckhoute J, et al. Rev-erb-α modulates skeletal muscle oxidative capacity by regulating mitochondrial biogenesis and autophagy. Nat Med 2013;19:1039–46. Crossref
27. Randolph LM, Jackson HA, Wang J, Shimada H, Sanchez-Lara PA, Wong DA, et al. Fatal infantile lactic acidosis and a novel homozygous mutation in the SUCLG1 gene: a mitochondrial DNA depletion disorder. Mol Genet Metab 2011;102:149–52. Crossref
28. Morava E, Steuerwald U, Carrozzo R, Kluijtmans LA, Joensen F, Santer R, et al. Dystonia and deafness due to SUCLA2 defect; Clinical course and biochemical markers in 16 children. Mitochondrion 2009;9:438–42. Crossref
29. Yu H, Kim PM, Sprecher E, Trifonov V, Gerstein M. The importance of bottlenecks in protein networks: correlation with gene essentiality and expression dynamics. PLoS Comput Biol 2007;3:e59. Crossref

DENEYSEL ÇALIŞMA - *ÖZET*

Yanık sıçanlarda mikrodizi analiziyle ortaya çıkartıldığı gibi erken akış fazında iskelet kaslarındaki IncRNA'ların ekspresyon imzaları

Dr. Zhang Haijun, Dr. Yu Yonghui, Dr. Chai Jiake

PLA Genel Hastanesi, Yanık ve Plastik Cerrahi Kliniği, Pekin, Çin

AMAÇ: Tüm vücut yüzeyinin (TVY) %30'dan fazlasını kaplayan ağır termal travma hipermetabolizma, kronik enflamasyon ve iskelet kaslarında güçsüzleşmeyi içermekle birlikte bu bulgularla sınırlı olmayan süregelen bir fizyopatolojik yanıtı da tetiklemektedir. Uzun zincirli proteini kodlamayan RNA'lar (lncRNA'lar) çeşitli biyolojik fonksiyonlara katılan, önemli ve yaygın bgenler sınıfıdır. Ancak ağır yanıklardan sonra iskelet kaslarının zayıflamasına ilişkin yanıtları düzenleyen RNA'ların fonksiyonları hâlâ test edilmemiştir.

GEREÇ VE YÖNTEM: Burada mikrodizi analizi kullanılarak, plasebo sıçanlarla karşılaştırmalı olarak erken akış fazında üç çift yanık sıçanın iskelet kası dokularındaki lncRNA'lar ve haberci RNA'ların (miRNA'lar) ekspresyon profilleri incelendi. Tanımlanmış her bir potansiyel lncRNA-mRNA çifti spesifik lncRNA-mRNA etkileşimlerin varlığının kesin olarak doğrulanmasında kullanılan ve yanık sıçanlarda iskelet kası zayıflamasının ayrıntılı bir patogenezini gösteren güçlü bir aday belirteçtir.

BULGULAR: Üç yaralı dokuyla eşleştirilmiş üç normal doku örneğinde mikrodizi analiz verileri kullanılarak LncRNA ekspresyon düzeyleri karşılaştırıldı. Ortalama 117 adet anlamlı derecede farklılaşmış lncRNA (1.5 katı) tanımlandı. Yalnızca 202 adet miRNA anlamlı derecede arttı veya azaldı. Eşleştirilmiş normal dokulara göre zedelenmiş dokularda ortalama 92 adet miRNA'nın düzeyleri artarken, ortalama 110 miRNA'nın düzeyleri azaldı.

TARTIŞMA: Burada, normal dokulara göre sıçanların yanık dokularında lncRNA'ların farklı düzeylerde eksprese edildiği saptanmıştır. İskelet kasları zayıflamasının patogenezinde düzenleyici yolaklar da rol oynayabilmektedir. Tanımlanmş her bir lncRNA-mRNA çifti spesifik lncRNA-miRNAA etkileşimlerinin varlığının doğrulanmasında kullanılan ve yanık sıçanlarda iskelet kası zayıflamasının ayrıntılı bir patogenezini gösteren güçlü bir aday belirteçtir.

Anahtar sözcükler: Ekspresyon; kas zayıflaması; LncRNA'lar; mikrodizi; yanık.

Ulus Travma Acil Cerrahi Derg 2016;22(3):224–232 doi: 10.5505/tjtes.2015.04831